Nano Energy (2012) 1, 448–455

Available online at www.sciencedirect.com

SciVerse ScienceDirect

journal homepage: www.elsevier.com/locate/nanoenergy

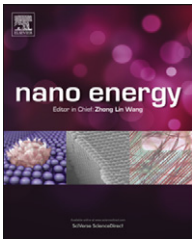

RAPID COMMUNICATION

Direct octane fuel cells: A promising power for transportation

Mingfei Liu[a], YongMan Choi[b,1], Lei Yang[a], Kevin Blinn[a], Wentao Qin[a], Ping Liu[b], Meilin Liu[a,c,*]

[a]*School of Materials Science and Engineering, Center for Innovative Fuel Cell and Battery Technologies, Georgia Institute of Technology, Atlanta, GA 30332-0245, USA*
[b]*Chemistry Department, Brookhaven National Laboratory, Upton, NY 11973, USA*
[c]*World Class University (WCU) Program, UNIST, South Korea*

Received 1 February 2012; received in revised form 19 February 2012; accepted 19 February 2012
Available online 3 March 2012

KEYWORDS
Fuel cells for transportation;
SOFC;
Multi-functional anode;
Coking tolerance;
Electric vehicles;
Reforming

Abstract
The demand for electric vehicles has inspired extensive efforts to develop solid oxide fuel cells (SOFCs) for transportation. However, the high cost of hydrogen fueled SOFC systems and the deactivation of Ni-YSZ anodes in hydrocarbon fuels hinder the progress of SOFCs' development and commercialization. Here, we report a unique multi-functional anode for SOFCs that allows direct utilization of transportation fuels (iso-octane) without co-feeding O_2 and CO_2, demonstrating a peak power density of ~0.6 W/cm^2 at 750 °C. The multi-functional anode is derived from a conventional NiO-YSZ anode with $BaCO_3$ modification in the anode support, creating a catalytically active conformal coating of $BaZr_{1-x}Y_xO_{3-\delta}$ (BZY) on YSZ and nano-islands of BaO on Ni surface, which greatly promote reforming of octane and oxidation of the reformed fuels. Further, the simple and cost-effective modification process can be readily adopted in the fabrication of the state-of-the-art NiO-YSZ supported cells.

Introduction

The desire for a clean and secure energy future has stimulated great interest in electric vehicles because the vehicles powered by conventional internal combustion engines have unacceptably low energy efficiency (only ~20%) in addition to emission of greenhouse gas and air pollutants. However, the transition to electric vehicles hinges on the development of a new generation of electrical energy storage and conversion systems such as batteries and fuel cells. While H_2-powered proton exchange

*Corresponding author: School of Materials Science and Engineering, Center for Innovative Fuel Cell and Battery Technologies, Georgia Institute of Technology, Atlanta, GA 30332-0245, USA. Tel.: +1 404 894 6114; fax: +1 404 894 9140.
E-mail addresses: mingfei.liu@mse.gatech.edu (M. Liu), meilin.liu@mse.gatech.edu (M. Liu).
[1]Present address: Chemical Catalysis Department, SABIC Technology Center in Riyadh, P.O Box 42503, Riyadh 11551, Saudi Arabia.

2211-2855/$ - see front matter © 2012 Elsevier Ltd. All rights reserved.
doi:10.1016/j.nanoen.2012.02.006

membrane (PEM) fuel cells [1] can efficiently convert H_2 to electricity with no emissions, the high cost to transport and store H_2 as well as its low volumetric energy density tarnishes the prospect for H_2-powered vehicles. Gasoline and diesel, in fact, have much higher volumetric and gravimetric energy density, are easy to handle, and allow for trouble-free refueling with the existing distribution system. Hence, gasoline or diesel-powered high-efficiency fuel cells would be ideally suited for electric vehicles.

Solid oxide fuel cells (SOFCs) based on an oxygen ion conductor such as yttria-stabilized zirconia (YSZ) hold great promise for direct utilization of the transportation fuels if the anodes have sufficient tolerance to coking and poisoning of the contaminants commonly encountered in these fuels [2–7]. Unfortunately, the conventional Ni-YSZ cermet anode in a state-of-the-art SOFC is prone to carbon deposition and deactivation in hydrocarbon fuels. Accordingly, alternative anode materials such as Cu-based cermet [8–10], $La_{0.75}Sr_{0.25}Cr_{0.5}Mn_{0.5}O_{3-\delta}$ [11], $Sr_2Mg_{1-x}Mn_xMoO_{6-\delta}$ ($0 \le x \le 1$) [12], doped (La,Sr)(Ti)O_3 [13,14], $La_{0.4}Sr_{0.6}Ti_{1-x}Mn_xO_{3-\delta}$ [15], and Ni-$BaZr_{0.1}Ce_{0.7}Y_{0.2-x}Yb_xO_{3-\delta}$ (Ni-BZCYYb) [3] have been developed for direct utilization of carbon-containing fuels. While these alternative anode materials have demonstrated some improved coking tolerance in light hydrocarbon fuels, they are still inefficient with liquid hydrocarbon fuels such as gasoline or diesel. Also, their practical application is stalled by other problems such as low electronic conductivity, poor electrochemical activity, and limited physical, chemical, and thermal compatibility with YSZ electrolyte at high temperatures during fabrication.

To retain the high-performance of Ni-based anodes while overcoming the susceptibility to coking, a thin catalytic coating (such as SDC [16–18], $SrZr_{0.95}Y_{0.05}O_{3-\delta}$ [19,20], Sn [21] or BaO [22]) has been introduced to modify the Ni surface or a porous catalyst layer (e.g., Ru-CeO_2 [23–26]) has been applied to the top of Ni-based anode to promote reforming of hydrocarbon fuels before they reach the Ni surface. Such catalytic coatings do not drastically alter the performance characteristics of the Ni-based anode, but greatly enhance its coking tolerance, even when iso-octane (a common surrogate for gasoline) is used as fuel [17,21,23–26]. It should be noted, however, that a large amount of CO_2 and/or O_2 must be co-fed with iso-octane to prevent coking. Past gas compositions for this purpose have included 5% iso-octane–9% air–86% CO_2 by Zhan et al. [23], humidified 3.9% iso-octane–96.1% air by Ding et al. [17], 6% iso-octane–94% air by Zhan et al. [25], and 5% iso-octane–9% air–3% H_2O–83% CO_2 by Sun et al. [24]. The excess amount of CO_2 and O_2 co-fed with fuel not only reduces the efficiency and increases the complexity of the system but also raise serious safety concerns. For example, the flammability range for iso-octane-air mixtures is 1.1–6% [17,23–25]. In particular, partial oxidation of iso-octane by O_2 is an exothermic reaction; the fast heating effect caused by the rapid oxidation reaction may become difficult to control. Further, the high cost of Ru may limit its practical application [23]. Thus, the development of a safe and cost-effective SOFC that can directly utilize automotive fuels such as gasoline would greatly accelerate the development of commercially viable electric vehicles.

Here we report a unique SOFC design based on a multi-functional anode, capable of directly utilizing transportation fuels without the addition of O_2 and/or CO_2. As schematically shown in Fig. 1(a), the anode consists of two layers: an outer catalyst layer for reforming of hydrocarbon fuels and an inner active anode layer in direct contact with the electrolyte for electrochemical oxidation of the reformed fuels. The outer catalyst layer, composed of Ni, YSZ, and $BaZr_{1-x}Y_xO_{3-\delta}$ (BZY) (Supplementary Fig. S1), was very effective for reforming of iso-octane without introducing any O_2 (air) and/or CO_2, which were required in previous studies [17,23–25] to avoid coking and anode deactivation.

Experimental

Fabrication of fuel cells

Button cells with a configuration Ni-YSZ-$BaZr_{1-x}Y_xO_{3-\delta}$ (and Ni-YSZ)|Ni-YSZ|YSZ|SDC|LSCF were fabricated in steps described as follows. First, an anode support with mixed NiO (Alfa), yttria-stabilized zirconia (8YSZ, Daiichi Kigenso, Japan) and $BaCO_3$ (Alfa) (weight ratio of 55:45:5) was fabricated by tape casting (~800 μm thick and pouched to ½ in. in diameter), followed by pre-firing at 850 °C for 2 h. Second, an active layer of NiO-YSZ (~15 μm) and a YSZ electrolyte (~15 μm) were sequentially deposited on the anode support by a particle suspension coating process followed by co-firing at 1400 °C for 5 h [27]. Third, a $Sm_{0.2}Ce_{0.8}O_{2-\delta}$ (SDC, synthesized by carbonate co-precipitation method [28]) buffer layer was deposited on YSZ surface and then LSCF (fuel cell materials) green tape fabricated by tape-casting process [29] was bonded onto the top of SDC buffer layer and co-fired with SDC at 1080 °C for 2 to form a porous cathode (~50 μm thick). The cathode area was 0.3 cm^2.

Electrochemical measurement

The cells were mounted onto an alumina tube using ceramic adhesive (Aremco, Ceramabond 552). NiO paste and silver paste (Heraeus) were applied as current collector for anode and cathode, respectively, and Ag wire as the lead for both electrodes. In order to avoid possible catalytic contribution of the paste, care was taken to ensure that no paste was on the active area of the anode. Humidified (3% H_2O) hydrogen was firstly fed into anode compartment to reduce the NiO in-situ, and ambient air was used as an oxidant. To evaluate the performance based on iso-octane, pure Argon at a flow rate of 15 ml/min was flowed through a bubbler containing pure iso-octane (Alfa) to entrain iso-octane at 25 °C (yielding ~6.5% iso-octane). Before entering the anode apartment, the mixture was humidified using water bubbler at 25 °C (3 vol% H_2O). The mixture corresponds to an H_2O to C_8H_{18} ratio of ~0.5, much lower than the ideal ratio for steam reforming of 8. The electrochemical testing of the cells was performed using an Arbin fuel cell testing system (MSTAT).

Other characterizations

The electrical conductivity of the anode (Ni-YSZ and Ni-YSZ-BZY) was measured using a four-electrode configuration at 500–800 °C under reducing conditions. The composition, microstructure, and morphology of the composite anode were analyzed using XRD (X'Pert PRO Alpha-1 x-ray diffractometer), SEM (LEO1530), high-resolution electron microscopy and

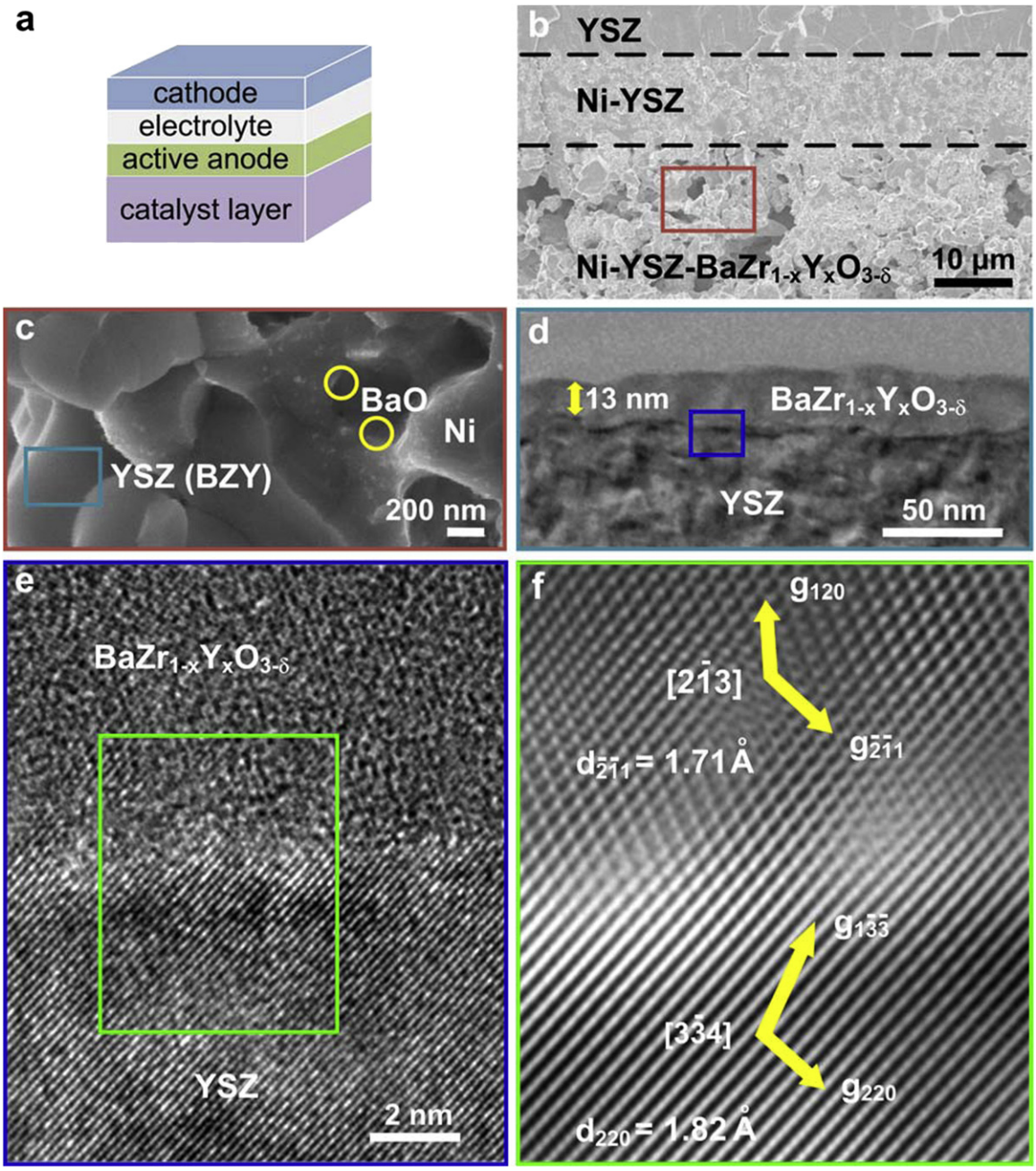

Figure 1 Architecture of a Ni-YSZ-BZY supported cell and microanalyses of the new anode. (a) Schematic of a unique SOFC design based on a multi-functional anode; (b) a typical cross sectional view of a Ni-YSZ-BZY supported porous Ni-YSZ active anode layer and a dense YSZ electrolyte (co-fired at 1400 °C C for 5 h; reduced in H_2 at 750 °C for 2 h); (c) a higher magnification of a small area in the Ni-YSZ-BZY layer (mechanical support and catalyst layer for reforming) shown in (b); (d) a cross-sectional view (TEM image) of a $BaZr_{1-x}Y_xO_{3-\delta}$ (BZY)-coated YSZ grain shown in (c); (e) HRTEM image of the interface between the BZY coating and the underlying YSZ. (f, g) Fourier-filtered images of the [2$\bar{1}$3] and [3$\bar{3}$4] zone axis images of BZY and YSZ near the interface, respectively.

spectroscopy (at Oak Ridge National Laboratory) and Raman spectroscopy (Renishaw 1000 with a 514 nm excitation wavelength). Mass spectrometry (Hiden HPR-20) was used to analyze the composition of the gas phase.

Computational methods

Density functional theory (DFT) calculations were carried out using the Vienna ab initio simulation package (VASP) [30,31] with the PW91 functional [32] and the projector augment wave (PAW) [33] method. We applied Monkhorst and Pack [34] mesh *k*-points of $(3 \times 3 \times 3)$ and $(4 \times 4 \times 1)$ for bulk and surface calculations, respectively, with the cut-off energy of 400 eV. Our predicted lattice constant of the cubic $BaZrO_3$ (BZ) structure ($Pm\bar{3}m$; 4.22 Å) is in agreement with experimental (4.19 Å) [35] and calculated (4.26 Å) [36] values. Based on the optimized BZ structure, we constructed a BZY ($Ba_{16}(Zr_{12}Y_4)O_{46}$) model to examine the interaction

between water and $BaZr_{1-x}Y_xO_{3-\delta}$ (BZY). For more detailed information, please refer to the supplementary content. The adsorption energies (E_{ads}) of water were calculated as follows:

$$E_{ads} = E[H_2O{-}BZY] - E[BZY] - E[H_2O]$$

where $E[H_2O\text{-surface}]$, $E[BZY]$, and $E[H_2O]$ are the predicted electronic energies for adsorbed H_2O on the BZY surface, the bare BZY surface, and gas-phase H_2O.

Results and discussion

The microstructure of this cell (Fig. 1b and c) appears similar to that of a state-of-the-art Ni-YSZ supported cell, as shown in Supplementary Fig. S2(a and b). The fabrication processes for the two types of cells are very similar as well; the only difference is that a small amount (~5 wt%) of $BaCO_3$ was added to the mixture of NiO and YSZ during the preparation of the catalyst layer, which is also used as the mechanical support for other cell components in the new cell design. Upon co-firing at 1400 °C for 5 h, the surface of the NiO-YSZ in the catalyst layer was modified by the $BaCO_3$ but not in the active layer (Supplementary Fig. S2c). SEM analyses of local microstructures and morphologies in the catalyst layer suggest that BaO nano particles were distributed on the Ni grains (Fig. 1c), as confirmed by EDS analysis (Supplementary Fig. S2d), while YSZ grains appear to be clean and smooth. A cross-sectional view of an YSZ grain (Fig. 1d) reveals a conformal surface coating (~13-20 nm thick) was formed on the YSZ grain surface. The composition of the surface coating is $BaZr_{1-x}Y_xO_{3-\delta}$ (BZY, with $x \approx 0.2$), as determined from X-ray photoelectron spectroscopy (Supplementary Fig. S3). This is also consistent with the XRD spectrum for the anode (Supplementary Fig. S1). An HRTEM image of the BZY/YSZ interface (Fig. 1e) suggests that YSZ in the field of view is a single crystal and some structural coherence exists between the two phases. The structural coherence is manifested as the alignment of the $(\bar{2}\,\bar{2}1)$ lattice fringes of $BaZr_{1-x}Y_xO_{3-\delta}$ with those of (220) of YSZ, as shown in the both the HRTEM image (Fig. 1e) and the Fourier-filtered image (Fig. 1f) of the interface between the $BaZr_{1-x}Y_xO_{3-\delta}$ and the underlying YSZ. The zone-axis and lattice fringes along the zone-axis of each phase along the interface are labeled in the Fourier-filtered image as well (Fig. 1f). It should be noted that the BaO nanoparticles on the Ni surface was resulted from reduction of $BaNiO_x$ upon exposure to a fuel, which was formed from reaction between NiO and $BaCO_3$ or BaO vapor decomposed from $BaCO_3$ during firing [22].

These analyses have shown that the surface modification of Ni-YSZ by $BaCO_3$ has produced a layer of discrete nano particles of BaO on the Ni surface and a conformal BZY coating on the YSZ surface. BZY is a good ionic conductor and can readily uptake water at elevated temperatures [37], similar to the BaO/Ni interfaces [22]. The water absorbed on the Ni-YSZ-BZY surface plays a vital role not only in promoting the octane reforming in the catalyst layer but also in facilitating water-mediated carbon removal [22] within the active anode layer of the fuel cell, thus achieving remarkable tolerance to coking and deactivation in heavy hydrocarbon fuels. In addition, alkali/alkaline-oxides, such as K_2O, CaO, SrO and BaO, have been known to be efficient additives in suppressing carbon deposition on conventional oxide-supported Ni catalysts for steam/CO_2 reforming processes [22,38-41]. The strong basicity of these oxides changes the metallic Ni surface to a slightly cationic state, reducing the ability of Ni to catalyze carbon formation from dehydration of hydrocarbon fuels. Further, these basic metal oxides themselves tend to adsorb the CO_2 produced by oxidation or reforming of carbon species, which further reduce the tendency for carbon deposition. As a result, the specific structure of BZY coated YSZ, together with discrete BaO nanoparticles on Ni surface, significantly enhance the tolerance to carbon deposition.

It should also be noted that some of these alkali/alkaline-oxides were introduced to Ni-YSZ anodes for SOFCs in an effort to enhance carbon tolerance [38,40,41]. For example, Jin et al. [19,20] infiltrated $SrZr_{0.95}Y_{0.05}O_{3-\delta}$(SZY) into Ni-YSZ anode to enhance the coking tolerance. However, their cell structure and performance are not comparable to ours and there are some limitations for practical application of their approach. While the alkaline oxide-modified Ni-YSZ anodes showed some improvement in coking tolerance in light hydrocarbon fuels such as methane, the power outputs of the fuel cells were much lower because of the poor electrical conductivity and the lack of microstructure optimizations.

While the effect of the surface modification by $BaCO_3$ on performance is dramatic, our fabrication procedure is simple and can be easily incorporated into an industrial process for fabrication of the state-of-the-art Ni-YSZ supported cells; the addition of small amount of $BaCO_3$ does not change the sintering behavior of the Ni-YSZ active anode layer or its compatibility with YSZ. While the conductivity of the Ni-YSZ-BZY composite is slightly lower than that of Ni-YSZ (Supplementary Fig. S4), the anode has relatively small sheet resistance because the anode layer is thick (~800 μm), functioning as an efficient current collector.

When humidified hydrogen was used as fuel, the new Ni-YSZ-BZY supported cell showed similar performance to that of a conventional Ni-YSZ supported cell, as shown in Fig. 2(a), achieving peak power densities of 1.09 and 1.16 W/cm^2 at 750 °C, respectively. However, the new cell configuration displayed much higher tolerance to coking in an octane fuel. Shown in Fig. 2(b) are the performances of a Ni-YSZ-BZY supported cell with wet (3 v% H_2O) iso-octane (6.5% in Ar) as fuel, demonstrating peak power densities of 0.6 and 0.1 W/cm^2 at 750 and 600 °C, respectively, comparable to those reported by Zhan et al. (~0.6 W/cm^2 at 770 °C and 0.1 W/cm^2 at 570 °C) using 5% iso-octane-9% air-86% CO_2 as fuel [23]. It is important to note that in the previous study [23], excess amounts of O_2 (or 9% air) and CO_2 (86%) were added to the octane fuel for partial oxidation and reforming in order to avoid coking and deactivation of the anode. In particular, the extra amount of O_2 in the mixture was vital to suppress carbon buildup on a conventional Ni-based anode. In our new cell design, by contrast, humidified (3% H_2O) iso-octane (6.5% in Ar), corresponding to a steam to carbon (S/C) ratio of 1/17 (much lower than the ideal reforming ratio of 1/1), was used as the fuel without addition of any O_2 and/or CO_2, dramatically reducing the system complexity, safety, and cost for fuel management. Stable cell operation was demonstrated with the wet iso-octane (6.5% in Ar) fuel for over 100 h without observable carbon deposition or

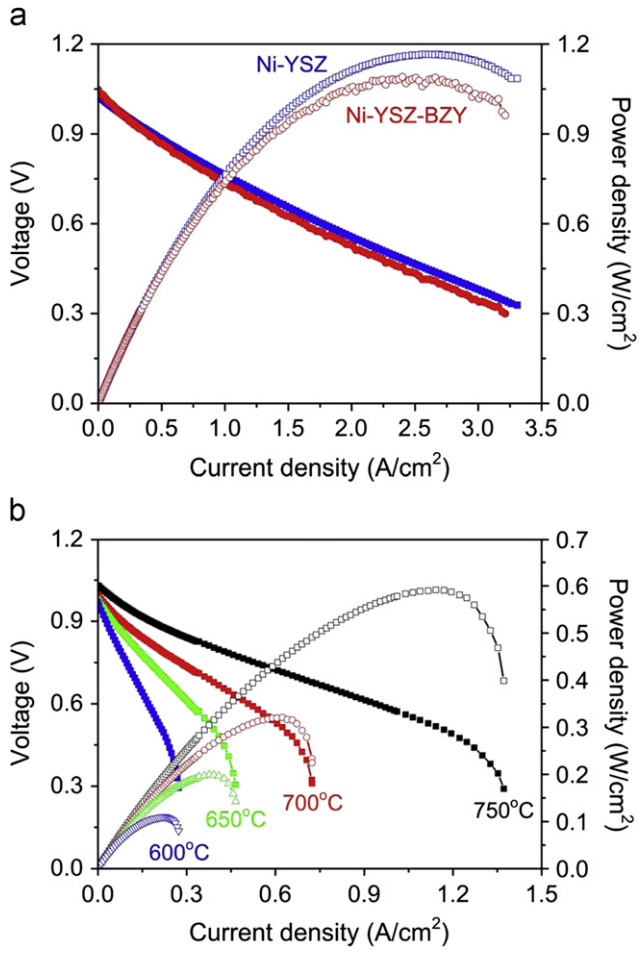

Figure 2 Performance of SOFCs in wet iso-octane. (a) Typical performance of a conventional Ni-YSZ supported cell and a Ni-YSZ-BZY supported cell when ambient air was used as oxidant and hydrogen as fuel. (b) Typical current–voltage characteristics and the corresponding power densities measured at 600–750 °C for cells supported by Ni-YSZ-BZY when ambient air was used as oxidant and wet so-octane (6.5% in Ar with 3 v% water vapor) as fuel. The performance was recorded after the cell reached a steady state operation (~20 h at 750 °C).

anode deactivation (Supplementary Fig. S5a). The observed direct utilization of a transportation fuel in an SOFC without the addition of excess O_2 and/or CO_2 is primarily attributed to the unique multifunctional anode structure: (i) the outer catalyst layer with BZY surface and BaO-modified Ni for reforming heavy hydrocarbons and water-mediated carbon removal and (ii) the inner active anode layer for electrochemical oxidation of the reformed fuels.

The stabilities of the two cells (supported by Ni-YSZ and Ni-YSZ-BZY) were examined under different conditions. Presented in Fig. 3 are the current densities drawn from each cell at a constant voltage of 0.7 V at 750 °C with the fuel switched from humidified H_2 to dry or wet iso-octane (6.5% in Ar). A stable power output was observed for the cell supported by Ni-YSZ-BZY with wet iso-octane (6.5% in Ar) as the fuel, achieving a relatively stable current density of ~0.56 A/cm^2 at 750 °C. In contrast, the current output of the conventional Ni-YSZ supported cell dropped to zero quickly due to severe carbon buildup on the Ni-YSZ anode,

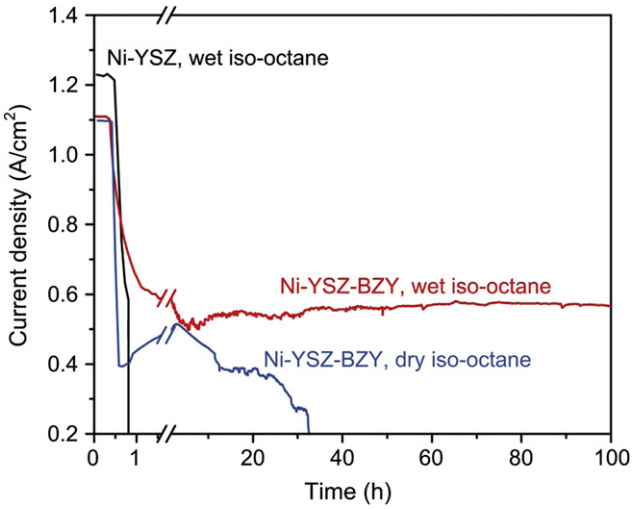

Figure 3 Fuel cell performance in different fuels. Current density as a function of time for the Ni-YSZ and Ni-YSZ-BZY supported cells operated at 750 °C at a constant cell voltage of 0.7 V as the fuel was switched from humidified H_2 to dry or wet iso-Octane (6.5% in Ar) (wet gas contained 3 v% water vapor as humidified at 25 °C).

which was visible under an optical microscope after the cell testing (Supplementary Fig. S5b). We also used Raman spectroscopy to probe an area on the Ni-YSZ anode that appeared to be relatively clean (Supplementary Fig. S5c) under the optical microscope and we found two peaks near 1350 and 1600 cm^{-1}, indicating the presence of carbon on the anode surface (Supplementary Fig. S6). In stark contrast, the Raman spectra collected from the anode surface of the Ni-YSZ-BZY-supported cell suggested that the anode surface was very clean and free of carbon (Supplementary Fig. S6). Careful examination of the anode microstructure of the Ni-YSZ-BZY supported cell before and after operation showed no observable carbon buildup or other changes in microstructure (Supplementary Fig. S7a and b), in contrast to the dramatic changes in anode morphology and microstructure of the conventional Ni-YSZ supported cell after operation under similar conditions.

It should be pointed out that sufficient amount of water co-fed with octane is needed to prevent coking. For example, the cell current degraded to zero (Fig. 3) after 40 h of operation at a constant voltage of 0.7 V when dry iso-octane (6.5% in Ar) was fed at a rate of 15 ml/min. At a constant current density of ~0.5 A/cm^2, the corresponding O^{2-} flux going through the electrolyte to the anode was $\sim 7.8 \times 10^{-7}$ mol/s (~0.52 ml/min of O_2), resulting in a nominal oxygen to carbon (O/C) ratio of 1/7.5 (O from O^{2-} flux and C from the iso-octane in the fuel stream). While high O^{2-} flux may prevent carbon formation near the triple phase boundary (TPB) area [42], it is ineffective to prevent carbon formation in the area far away from the TPB. When dry iso-octane is used as the fuel, the steam and/or CO_2 formed by fuel oxidation will be adsorbed on the anode surface, resulting in somewhat improved coking tolerance compared to the conventional Ni-YSZ anode. However, the initial exposure to dry iso-octane has high probability of promoting carbon deposition. It appears that a minimum O/C or S/C ratio may be necessary to suppress carbon

deposition from thermal cracking of iso-octane. As pointed out by Zhan et al. [23], a small amount of air in the iso-octane was required to fully stabilize the performance even though a large amount of excess CO_2 (6% iso-octane–94% CO_2) was used.

The dramatically enhanced catalytic activity of the Ni-YSZ-BZY compared to Ni-YSZ might result from the specific feature of the microstructure: discrete nano particles of BaO on the Ni surface and a conformal BZY coating on the YSZ surface. The two features can readily uptake water at elevated temperatures [22,37]. When a small amount of water was co-fed with iso-octane in the fuel stream, the water vapor was more easily be adsorbed and/or absorbed on BZY and BaO/Ni to facilitate reformation of iso-octane or decomposed species such as ethane and methane. Because of the strong adsorption of water on surfaces, the O/C or S/C ratio near the surface may have been sufficiently higher than that in the gas phase to avoid coking.

To gain some insight into water intake on BZY at microscopic level, we performed DFT calculations using the Vienna ab initio simulation package (VASP) [30,31] and constructed a defective $Ba_{16}(Zr_{12}Y_4)O_{46}$ (BZY) with two oxygen vacancies, derived from a defective $Ba_8(Zr_6Y_2)O_{23}$ model (Supplementary Fig. S8). As described in more detail in the Supplementary Information, the (001) surface was used to calculate water adsorption energy. Due to the presence of an oxygen vacancy, four types of terminated layers (i.e., BaO-I, BaO-II, ZrYO-I, and ZrYO-II) have been considered. Our surface stability calculations (Supplementary Fig. S9) show that the BaO-I- and ZrYO-I-terminations are more stable than the others with surface energies of 0.42 and 0.41 J/m^2, respectively. Depending on adsorption sites (i.e., metal, oxygen, or oxygen vacancies), water can be adsorbed via either molecular or dissociative adsorption [43] on the BZY surfaces with both BaO-I- and ZrYO-I-terminations. Shown in Fig. 4 is the geometrical illustration of dissociative adsorption of water on the BZY surfaces. Similar to water dissociation on BaO(001) and $BaZrO_3$(001) (E_{ads} = −1.35 eV and −1.25 eV, respectively) [22], one of O-H bonds of water can be broken without a barrier on the BZY surfaces (E_{ads} = −1.82 eV and −1.61 eV on BaO- and ZrYO-terminated surfaces, respectively), which is a highly activated process on Ni. Our calculations are in accordance with the experimental finding that BZY can readily uptake water. We used thermogravimetric analysis (TGA) and Raman spectroscopy to validate this theoretical calculation. Both TGA (Supplementary Fig. S10) and Raman results (Supplementary Fig. S11) demonstrated that BZY has strong water uptake ability even at high temperatures when it was exposed to water contained atmosphere. In addition, Bader charge calculations [44] show that electron transfer occurs from the surface to adsorbed water (−0.80*e* versus −0.84*e*, respectively), resulting in barrierless H-OH bond breaking (1.66 Å versus 2.03 Å, respectively). Our DFT calculations suggest that similar to BaO, BZY formed on the YSZ electrolyte surface engenders the synergetic effect with Ni by releasing the bottleneck OH production on the Ni anode [22], and therefore promoting the iso-octane reforming and the removal of carbon species on Ni ($OH^*_{BZY} \rightarrow OH^*_{Ni}$, $OH^*_{Ni} + C^*_{Ni} \rightarrow COH^*_{Ni} \rightarrow CO^*_{Ni} + H^*_{Ni}$, where "*" denotes surface empty sites).

Finally, mass spectrometry was used to analyze the composition of the effluent gas from the cell operated at a constant voltage of 0.7 V as the operating temperature was varied from 600 to 750 °C, which helps us to better understand the reactions taking place in the anode. At 750 °C, iso-octane was almost completely converted to C_2H_4, H_2, CH_4, H_2O, CO, and CO_2 (Supplementary Figs. S12 and S13) through cracking, reformation, and electrochemical oxidation. Thermodynamic and experimental analyses by Murray et al. indicated that iso-octane was primarily converted to ethylene and methane at 775 °C, while part of the ethylene and methane was consumed under SOFC operating condition at constant cell voltage of 0.5 V [45]. Shown in Fig. 5 are the concentration profiles of the effluent gas from a Ni-YSZ-BZY supported cell as a function of operating temperature. The concentration of CO_2 remained relatively low and constant in the temperature range studied, indicating that the rate of electrochemical oxidation and/or reforming of carbon species to CO_2 were relatively low. The concentration of H_2O increased significantly with temperature due to the corresponding increase in current density (oxygen flux) or electrochemical oxidation of H_2 and C_2H_4 with temperature. Thus, the concentrations of H_2 and C_2H_4 decreased with temperature accordingly. It is noted that the cell operated under low fuel utilization is more susceptible to coking because the tendency for coking decreases with fuel utilization when more oxidation products (CO_2 and H_2O) are produced in the anodic compartment. The stable operation observed in the temperature range of 600–750 °C (Fig. 3 and Supplementary Fig. S14, Uf < 5% and Supplementary Fig. S15, Uf < 1%) indicated that the anode catalyst layer of Ni-YSZ-BZY displays sufficient tolerance to coking. Further, it is noted that this multi-functional anode also demonstrated high

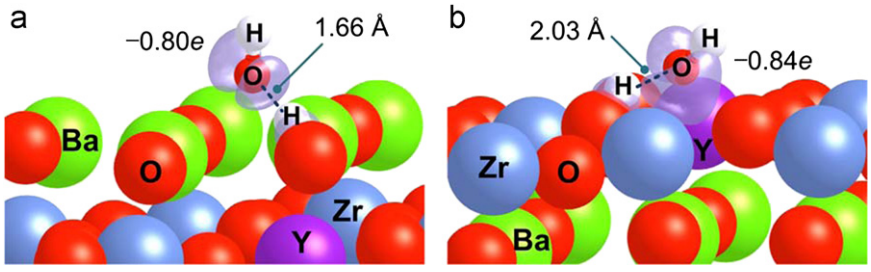

Figure 4 Dissociative adsorption of water on the BaO- and ZrYO-terminated surfaces of $Ba_{16}(Zr_8Y_4)O_{46}$ (BZY)—a vital step for water-mediated carbon removal. For simplicity, only two top layers were shown. Large balls in green, gray blue, purple, red are Ba, Zr, Y, and O ions of BZY, while small balls in white and red are H and O atoms of H_2O. Dashed lines represent the broken O-H bond. $\Delta\rho_{diff}$ isosurfaces were calculated at 0.05 e/Å^3.

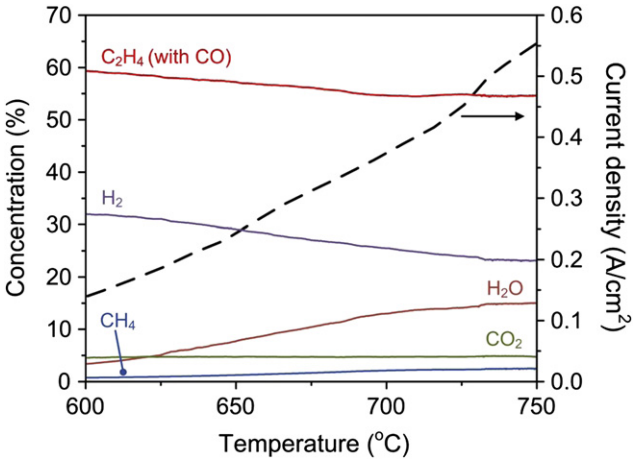

Figure 5 Effect of temperature on internal reforming of iso-octane. Concentration profile (as determined by a mass spectrometer, Ar was removed from the calculation) of the effluent gas from the Ni-YSZ-BZY supported cell as a function of operating temperature. The cell was operated at a constant voltage of 0.7 V when wet iso-octane (6.5% in Ar) at a flow rate of 15 mL/min was used as the fuel and ambient air as the oxidant.

tolerance to sulfur poisoning under typical fuel cell operating conditions; more results on sulfur poisoning behavior of the Ni-YSZ-BZY layer will be reported in subsequent communications.

Conclusions

A multi-functional composite anode, derived from a conventional NiO-YSZ anode with $BaCO_3$ modification in the anode support, showed potential for direct utilization of transportation fuels such as iso-octane without the addition of excess amount of CO_2 and/or O_2, demonstrating peak power densities of 0.6 and 0.1 W/cm^2 at 750 and 600 °C, respectively. The unique properties of the bi-layer anode are attributed to the nanostructured BZY coating on the YSZ phase and the BaO nanoparticles on the Ni surface of the composite anode. The desirable nanostructures can be created by a simple and cost-effective modification of the existing processes for fabrication of the state-of-the-art SOFCs based on YSZ electrolyte. High-performance fuel cells that run on transportation fuels hold great promise for electric and hybrid electric vehicles.

Acknowledgments

This material is based upon work supported as part of the Heterogeneous Functional Materials (HetroFoaM) Center, an Energy Frontier Research Center funded by the U.S. Department of Energy (DOE), Office of Science, Office of Basic Energy Sciences under Award Number DE-SC0001061. The authors would like to acknowledge the use of Oak Ridge National Laboratory's SHaRE User Facility, which is sponsored by the Scientific User Facilities Division, Office of Basic Energy Sciences, Office of Science, the U.S. Department of Energy. Partial support of the WCU program at UNIST, South Korea, is also acknowledged. We thank Dr. Karren More and Ms. Dorothy Coffey of SHaRE, ORNL for TEM instrumentation support and TEM sample preparation, respectively. DFT calculations were performed at Brookhaven National Laboratory, supported by the U.S. DOE, BES, under Contract no. DE-AC02-98CH10886, using the computational facilities at the National Energy Research Scientific Computing Center (Contract No. DE-AC02-05CH11231).

Appendix A. Supporting information

Supplementary data associated with this article can be found in the online version at doi:10.1016/j.nanoen.2012.02.006.

References

[1] B.C.H. Steele, A. Heinzel, Nature 414 (2001) 345–352.
[2] M. Liu, M.E. Lynch, K. Blinn, F.M. Alamgir, Y. Choi, Materials Today 14 (2011) 534–546.
[3] L. Yang, S.Z. Wang, K. Blinn, M.F. Liu, Z. Liu, Z. Cheng, M.L. Liu, Science 326 (2009) 126–129.
[4] A. Atkinson, S. Barnett, R.J. Gorte, J.T.S. Irvine, A.J. Mcevoy, M. Mogensen, S.C. Singhal, J. Vohs, Nature Materials 3 (2004) 17–27.
[5] B.C.H. Steele, Nature 400 (1999) 619.
[6] Z. Cheng, J.H. Wang, Y.M. Choi, L. Yang, M.C. Lin, M.L. Liu, Energy and Environmental Science 4 (2011) 4380–4409.
[7] X. Li, K. Blinn, Y. Fang, M. Liu, S. Cheng, M.A. Mahmoud, L.A. Bottomley, M. El-Sayed, M. Liu, Physical Chemistry Chemical Physics (2012). doi:10.1039/c2cp40091j.
[8] S.D. Park, J.M. Vohs, R.J. Gorte, Nature 404 (2000) 265–267.
[9] R.J. Gorte, J.M. Vohs, Journal of Catalysis 216 (2003) 477–486.
[10] C. Lu, W.L. Worrell, R.J. Gorte, J.M. Vohs, Journal of the Electrochemical Society 150 (2003) A354–A358.
[11] S.W. Tao, J.T.S. Irvine, Nature Materials 2 (2003) 320–323.
[12] Y.H. Huang, R.I. Dass, Z.L. Xing, J.B. Goodenough, Science 312 (2006) 254–257.
[13] M.R. Pillai, I. Kim, D.M. Bierschenk, S.A. Barnett, Journal of Power Sources 185 (2008) 1086–1093.
[14] M.R. Pillai, Y. Jiang, N. Mansourian, I. Kim, D.M. Bierschenk, H.Y. Zhu, R.J. Kee, S.A. Barnett, Electrochemical and Solid-State Letters 11 (2008) B174–B177.
[15] Q.X. Fu, F. Tietz, D. Stover, Journal of the Electrochemical Society 153 (2006) D74–D83.
[16] W. Zhu, C.R. Xia, J. Fan, R.R. Peng, G.Y. Meng, Journal of Power Sources 160 (2006) 897–902.
[17] D. Ding, Z.B. Liu, L. Li, C.R. Xia, Electrochemistry Communications 10 (2008) 1295–1298.
[18] L.S. Zhang, J.F. Gao, M.F. Liu, C.R. Xia, Journal of Alloys and Compounds 482 (2009) 168–172.
[19] Y.C. Jin, H. Saito, K. Yamahara, M. Ihara, Electrochemical and Solid-State Letters 12 (2009) B8–B10.
[20] Y.C. Jin, H. Yasutake, K. Yamahara, M. Ihara, Journal of the Electrochemical Society 157 (2010) B130–B134.
[21] E. Nikolla, J. Schwank, S. Linic, Journal of the Electrochemical Society 156 (2009) B1312.
[22] L. Yang, Y. Choi, W. Qin, H. Chen, K. Blinn, M. Liu, P. Liu, J. Bai, T.A. Tyson, M. Liu, Nature Communications 2 (2011) 357.
[23] Z.L. Zhan, S.A. Barnett, Science 308 (2005) 844–847.
[24] C.W. Sun, Z. Xie, C.R. Xia, H. Li, L.Q. Chen, Electrochemistry Communications 8 (2006) 833–838.
[25] Z.L. Zhan, S.A. Barnett, Journal of Power Sources 157 (2006) 422–429.
[26] Z.L. Zhan, S.A. Barnett, Journal of Power Sources 155 (2006) 353–357.

[27] M.F. Liu, D.H. Dong, R.R. Peng, J.F. Gao, J. Diwu, X.Q. Liu, G.Y. Meng, Journal of Power Sources 180 (2008) 215–220.
[28] D. Ding, B. Liu, Z. Zhu, S. Zhou, C. Xia, Solid State Ionics 179 (2008) 896–899.
[29] L.F. Nie, Z. Liu, M.F. Liu, L. Yang, Y.J. Zhang, M.L. Liu, Journal of Electrochemical Science and Technology 1 (2010) 50–56.
[30] G. Kresse, J. Hafner, Physical Review B 47 (1993) 558–561.
[31] G. Kresse, J. Furthmuller, Physical Review B 54 (1996) 11169–11186.
[32] J.P. Perdew, Y. Wang, Physical Review B 45 (1992) 13244–13249.
[33] P.E. Blöchl, Physical Review B 50 (1994) 17953–17979.
[34] H.J. Monkhorst, J.D. Pack, Physical Review B 13 (1976) 5188–5192.
[35] S. Yamanaka, M. Fujikane, T. Hamaguchi, H. Muta, T. Oyama, T. Matsuda, S.-i. Kobayashi, K. Kurosaki, Journal of Alloys and Compounds 359 (2003) 109–113.
[36] M.A. Gomez, M. Chunduru, L. Chigweshe, L. Foster, S.J. Fensin, K.M. Fletcher, L.E. Fernandez, Journal of Chemical Physics 132 (2010) 214709.
[37] Y. Yamazaki, P. Babilo, S.M. Haile, Chemistry of Materials 20 (2008) 6352–6357.
[38] T. Takeguchi, Y. Kani, T. Yano, R. Kikuchi, K. Eguchi, K. Tsujimoto, Y. Uchida, A. Ueno, K. Omoshiki, M. Aizawa, Journal of Power Sources 112 (2002) 588–595.
[39] T. Horiuchi, K. Sakuma, T. Fukui, Y. Kubo, T. Osaki, T. Mori, Applied Catalysis, A 144 (1996) 111–120.
[40] D. La Rosa, A. Sin, M. Lo Faro, G. Monforte, V. Antonucci, A.S. Arico, Journal of Power Sources 193 (2009) 160–164.
[41] M. Asamoto, S. Miyake, K. Sugihara, H. Yahiro, Electrochemistry Communications 11 (2009) 1508–1511.
[42] S. McIntosh, R.J. Gorte, Chemical Reviews 104 (2004) 4845–4865.
[43] A.V. Bandura, R.A. Evarestov, D.D. Kuruch, Surface Science 604 (2010) 1591–1597.
[44] G. Henkelman, A. Arnaldsson, H. Jónsson, Computational Materials Science 36 (2006) 254–360.
[45] E.P. Murray, S.J. Harris, J. Liu, S.A. Barnett, Solid-State Letters 9 (2006) A292–A294.

Mingfei Liu is a postdoctoral fellow in the School of Materials Science and Engineering at the Georgia Institute of Technology, USA. He received his BS and Ph.D. from the University of Science and Technology of China (USTC). His research interests include developing novel electronic and ionic conductors for energy storage and conversion (e.g., fuel cells, batteries, electro-catalysis/synthesis) and fundamental understanding of electrode properties, particularly cathodes and anodes for solid oxide fuel cells. His technical expertise includes fabrication and evaluation of ceramic membranes, thin films, and coatings; design, fabrication, and testing of meso-porous and nano-structured electrodes and devices for energy storage and conversion.

YongMan Choi is a Lead Scientist in the Chemical Catalysis Department at SABIC Technology Center in Riyadh, Saudi Arabia. He received his Ph.D. in Chemistry from Emory University (Georgia, USA) under the guidance of Professor M.C. Lin, after obtaining his B.S. and M.S. from Ajou University in Korea, and worked as a research engineer in the Institute for Advanced Engineering. Before joining SABIC, he was a research associate in the Chemistry Department at Brookhaven National Laboratory (New York, USA), and a postdoctoral fellow in the School of Materials Science and Engineering at Georgia Institute of Technology (Georgia, USA). His research interests include fuel cells, hydrogen production, and fuel synthesis. He currently focuses on designing novel materials for heterogeneous catalysis, photocatalysis, and photoelectrocatalysis.

Lei Yang is currently a research scientist at ConocoPhillips Company pursuing research in the area of efficient energy devices. He received his Ph.D. in Materials Science and Engineering (2011) from Georgia Institute of Technology, and his M.S. in Materials Physics and Chemistry (2006) from Tsinghua University, China. His research interests include solar cells, fuel cells, batteries, and super-capacitors, especially the design of novel materials and nanoscale architectures, the development of new methods for understanding surface reaction and transport phenomena, and the exploration of optimal approaches for cost-effective assembly of energy devices.

Kevin Blinn is a Ph.D candidate in the School of Materials Science and Engineering at the Georgia Institute of Technology. He works for Prof. Meilin Liu's group, which he joined in 2007 after receiving a Bachelor's degree in Ceramic and Materials Engineering from Rutgers University. His current thesis research involves the use of optical spectroscopy to characterize the transport phenomena and stability of solid oxide fuel cell (SOFC) cathodes and anodes in order to aid the development of better electrode materials. Other research interests include the development of energy storage and conversion methods for aeronautical and aerospace applications.

Wentao Qin was a postdoctoral fellow in Professor Meilin Liu's group at Georgia Institute of Technology, and currently a materials scientist and the primary TEM microscopist in ON Semiconductor, Phoenix, Arizona, USA. He received his B.S. from the University of Science and Technology of China in Hefei, China, and Ph.D. from the University of Missouri-Rolla, USA. Wentao's PhD thesis focused on 3-dimensdional crystallography of nanocrystals via high-resolution TEM. His research interest includes materials characterization and structure–property correlation for advanced electrode materials in solid oxide fuel cells, super-capacitors, and semiconductor electronic devices.

Meilin Liu is a Regents' Professor of Materials Science and Engineering and Co-Director of the Center for Innovative Fuel Cell and Battery Technologies at Georgia Institute of Technology, Atlanta, Georgia, USA. He received his BS from South China University of Technology and MS and Ph.D. from the University of California at Berkeley. His research interests include *in situ* characterization and multi-scale modeling of charge and mass transfer along surfaces, across interfaces, and in membranes, thin films, and nanostructured electrodes, aiming at achieving rational design of materials and structures with unique functionalities for efficient energy storage and conversion.